UNIVERSITY OF MINNESOTA
Driven to Discover®

Development of new concept antenna (Mono-Dipole) array for human head imaging at 10.5T

Myung Kyun Woo[1], Lance DelaBarre[1], Russell L Lagore[1], Andrea Grant[1], Yigitcan Eryaman[1], Jerahmie Radder[1], Xiaoping Wu[1], Pierre-Francois Van de Moortele[1], Edward Auerbach[1], Greg Metzger[1],Kamil Ugurbil[1] and Gregor Adriany[1]

[1]Center for Magnetic Resonance Research (CMRR), University of Minnesota, Minneapolis, MN, United States

Motivation and Objective: As a transmitter, a 16 channel (CH) dipole head array is desirable above 7T, however, it is difficult to achieve this high channel count due to coupling [1-3]. Shortening the length of the dipole is also required for human head applications [4, 5]. We explore the potential of a novel 16 CH Mono-Dipole head array to achieve improved B_1^+ field uniformity and intra-element decoupling. To investigate this, we first compared an 8 CH end-loaded dipole array and a Mono-Dipole array in simulation and verified B_1^+ experimentally [6]. We then compared arrays of 16 CH Mono-Dipole and closer fitting Stripline arrays for achievable B_1^+ field efficiency at 10.5T.

Methods: The 16 CH transceiver Mono-Dipole head array is shown in Fig. 1. The coil was effectively shortened to a common RF ground using 680 pF capacitors in Fig. 2. Floating cable traps were used to suppress the cable sheath currents [7].

Electromagnetic simulations were performed in XFdtd (REMCOM, State College, PA) to calculate the B_1^+ field (normalized to 1 W). The B_1^+ efficiency was initially compared with 8 CH Dipole array and Mono-Dipole array of the same dimensions (Fig. 3). Transmit B_1^+ profiles obtained using an actual flip angle imaging (AFI) sequence for a cylindrical phantom (17 cm diameter, 30.5 cm height) are also shown in Fig 3. The phantom has uniform electrical properties (σ= 0.6 S/m, ε_r = 49). Fig. 4 shows the experimentally acquired individual transmit fields of the Mono-Dipole array. Fig. 5 shows the experimental results of the comparison between the arrays of 16 CH Stripline (20 × 22 cm²) and Mono-Dipole (24 × 24 cm²). Fig. 6 shows the simulation result of the 16 CH Mono-Dipole array with a human model (Duke).

Results: Excellent agreement between simulations and experiments (within 10%) was achieved for the highest B_1^+ values among the 8 CH end-loaded dipole and the Mono-Dipole arrays in Fig. 2. Individual element performance of the 16 CH Mono-Dipole array is shown in Fig. 3. Coupling of the 16CH Mono-Dipole array is on the order of -9 ~ -11 dB between the next nearest neighbors. From AFI imaging, the transmit efficiency of the Stripline array (0.51 μT/ √W) was lower than the Mono-Dipole array (0.59 μT/√W) in Fig. 5. Even though the dimension of Stripline array has a 20% smaller area than the Mono-dipole array, Mono-Dipole array shows higher B_1^+efficiency compared to the Stripline array.

Conclusion: Improved decoupling between channels is observed in the Mono-Dipole arrays. For the 16 CH Mono-Dipole array, phase shimming between elements is required for optimized results. We observed that 16 CH Mono-Dipole head antenna array has potential advantages for whole head coverage at 10.5T.

References: [1] Connell I., ISMRM p. 4295 (2017)
[2] Gilbert K. ISMRM p. 2661 (2017)
[3] Lattanzi R. MRM DOI: 10.1002/mrm.26803 (2017)
[4] Chen G. MRM DOI 10.1002/mrm.26777 (2017)
[5] Chen G. ISMRM-ESMRMB p. 621 (2014)
[6] Lagore R. ISMRM p. 1051 (2016)
[7] SEEBER D. Concepts Magn Reson 21B: 26–31, 2004

Acknowledgements: NIH- U01 EB025144 S10 RR026783, BTRC P41 EB015894, P30 NS076408 and WM Keck Foundation

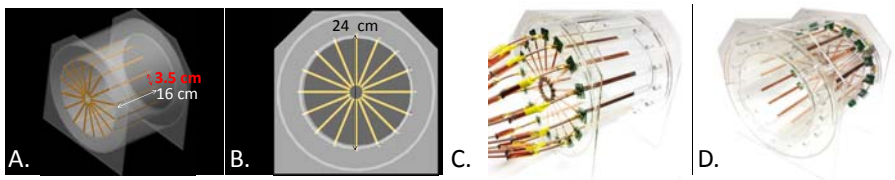

Figure 1. 3D CAD Rendering (A and B) and Photographs (C and D) of the 16 CH Mono-Dipole array

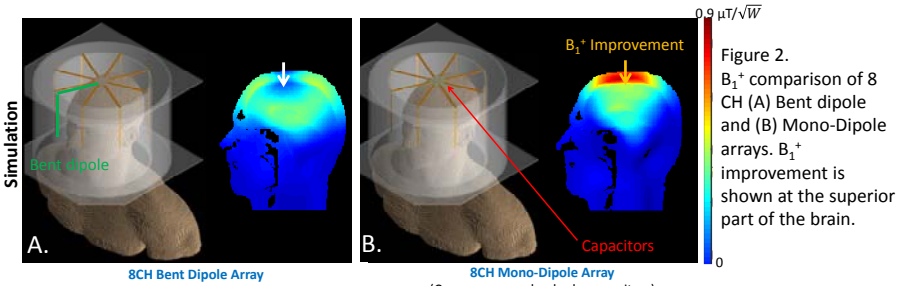

Figure 2. B_1^+ comparison of 8 CH (A) Bent dipole and (B) Mono-Dipole arrays. B_1^+ improvement is shown at the superior part of the brain.

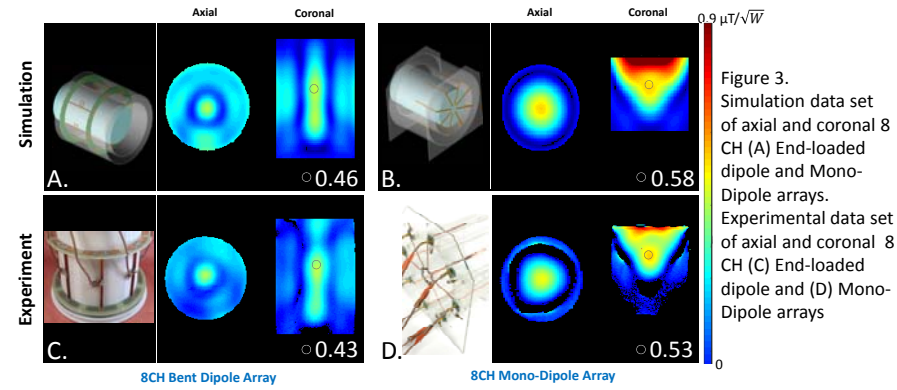

Figure 3. Simulation data set of axial and coronal 8 CH (A) End-loaded dipole and Mono-Dipole arrays. Experimental data set of axial and coronal 8 CH (C) End-loaded dipole and (D) Mono-Dipole arrays

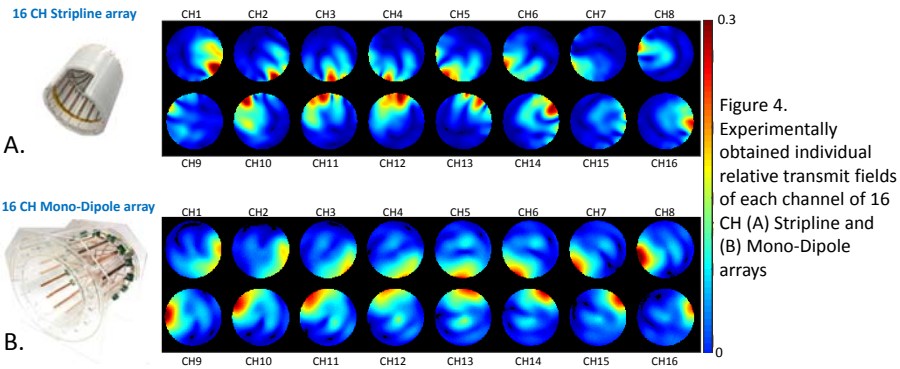

Figure 4. Experimentally obtained individual relative transmit fields of each channel of 16 CH (A) Stripline and (B) Mono-Dipole arrays

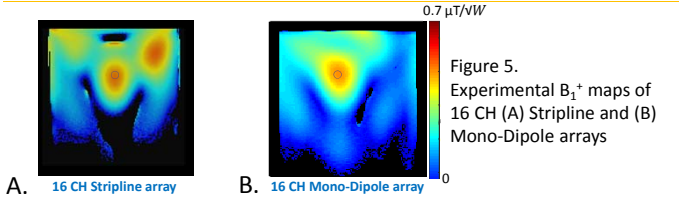

Figure 5. Experimental B_1^+ maps of 16 CH (A) Stripline and (B) Mono-Dipole arrays

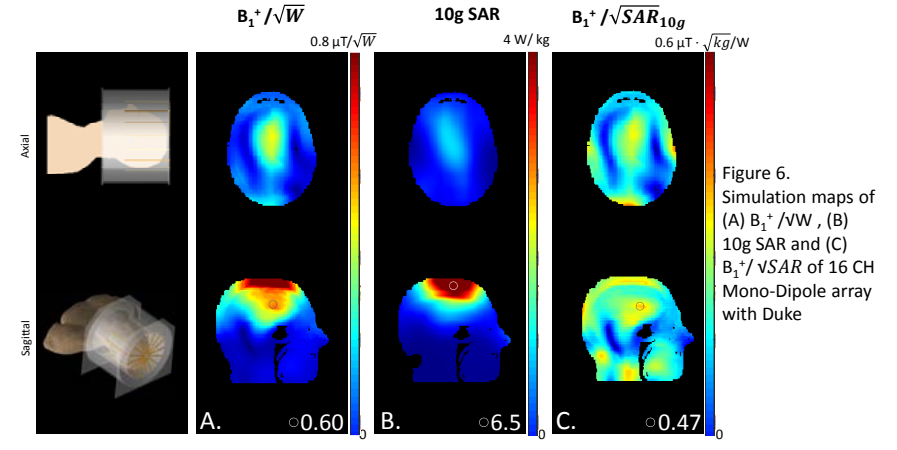

Figure 6. Simulation maps of (A) $B_1^+/\sqrt{W}$, (B) 10g SAR and (C) $B_1^+/\sqrt{SAR}$ of 16 CH Mono-Dipole array with Duke